Contents lists available at GrowingScience

Current Chemistry Letters

homepage: www.GrowingScience.com

Molecular docking against Covid-19 and HIV, and the role of catalysis in stereoselective cycloaddition reactions: A theoretical investigation of TiCl4-promoted reactions between cyclopenta-1,3-diene and benzyl acrylate/benzyl 2-fluoroacrylate

Khadija El Idrissi[a,b], Abdellah Zeroual[a*] and Hocine Garmes[b]

[a]*Molecular Modelling and Spectroscopy Research Team, Faculty of Science, Chouaïb Doukkali University, P.O. Box 20, 24000 El Jadida, Morocco*
[b]*Analytical Chemistry and Environmental Sciences Team, Department of chemistry, Faculty of Science, University Chouaib Doukkali, El Jadida, Morocco*

C H R O N I C L E

Article history:
Received August 3, 2024
Received in revised form
September 16, 2024
Accepted November 9, 2024
Available online
November 9, 2024

Keywords:
MEDT
Stereoselective
SARS-Covid-19
HIV
Kinetic control
ELF

A B S T R A C T

The study of cycloaddition reactions between cyclopenta-1,3-diene and benzyl-acrylate, as well as benzyl-2-fluoroacrylate with and without the catalyst (TiCl4), was conducted using MEDT. The results of the energy profiles suggest that these reactions are stereoselective, meaning that they favor the formation of certain stereoisomers over others. Furthermore, the addition of TiCl4 as a catalyst appears to enhance the selectivity of these reactions, which is in line with experimental observations. Additionally, a docking study was carried out to predict the effect of stereochemistry and the presence of specific atoms, such as fluorine, on their ability to bind to viral proteins responsible for SARS-Covid-19 and HIV. Moreover, the notable affinity of Ligand 4 for HIV renders it a pivotal contender for extended research, possibly paving the way for enhanced antiretroviral drugs. Similarly, the encouraging affinity demonstrated by Ligand 1 towards the Covid-19 protein highlights its promise for Covid-19 drug development.

1. Introduction

Bicyclic products are of biological interest because of their ability to interact specifically with biological targets, their structural stability, and their pharmacological properties[1]. For example, many drugs, such as certain antibiotics, anti-inflammatory drugs or anticancer agents, are bicyclic compounds[2]. Some bicyclic products can mimic the structure of important natural molecules in organisms[3]. This can lead to a specific interaction with proteins or other cellular components, resulting in specific biological effects - the reason why bicyclic compounds are often used in medicinal chemistry to design molecules with specific properties, improving drug efficacy, selectivity and bioavailability[4]. Research into these compounds can open up prospects for the development of new drugs or biologically active compounds based on cycloaddition reactions [2+4][5].

[4+2] cycloaddition reactions are chemical processes in which two reactants, one of them containing two reactive atoms (dienophile) and the other containing four reactive atoms (diene), react to form a six-membered cyclic compound[6]. The [4+2] cycloaddition reaction is often associated with the Diels-Alder reaction. In the Diels-Alder reaction, a diene can react with a cyclic dienophile to form a bicyclic compound (**Scheme 1**).

* Corresponding author
E-mail address zeroualabdellah2@gmail.com (A. Zeroual)

doi: 10.5267/j.ccl.2024.11.006

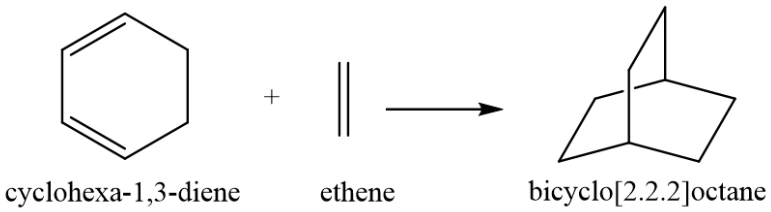

Scheme 1

The substitution of fluorine atoms for bicyclic compounds represents a promising strategy in the synthesis of drugs or biologically active compounds[7]. Incorporating fluorine atoms into bicyclic structures offers several advantages, including improved chemical stability, modulation of physicochemical properties, and increased affinity for biological targets[8]. Fluorine, due to its small size and high electronegative power, can significantly influence the chemical reactivity of compounds, leading to potentially more therapeutically effective products[9]. This fluorine substitution approach to the design of bicyclic compounds reflects a growing trend in medicinal chemistry to optimize the pharmacological properties and bioavailability of active substances, opening up new prospects for the development of innovative therapies[10, 11]. In this context, Lam et al have synthesized bicyclic compounds by reacting cyclopenta-1,3-diene with benzyl acrylate and benzyl 2-fluoroacrylate (**Scheme 2**)[12].

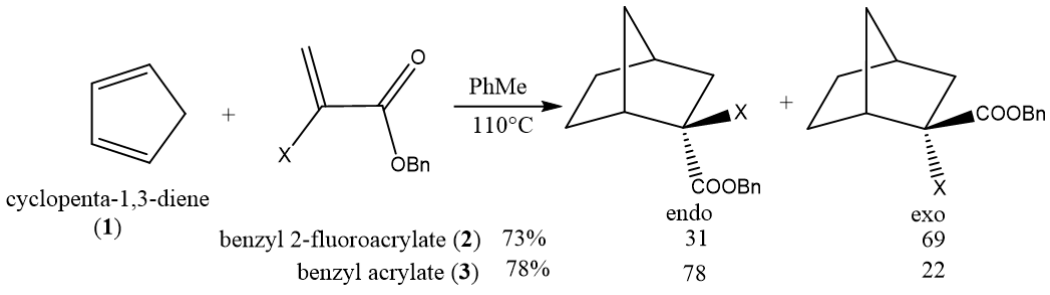

Scheme 2

These reactions are stereoselective, and the use of catalysts such as Lewis acids makes them stereospecific (**Scheme 3**).

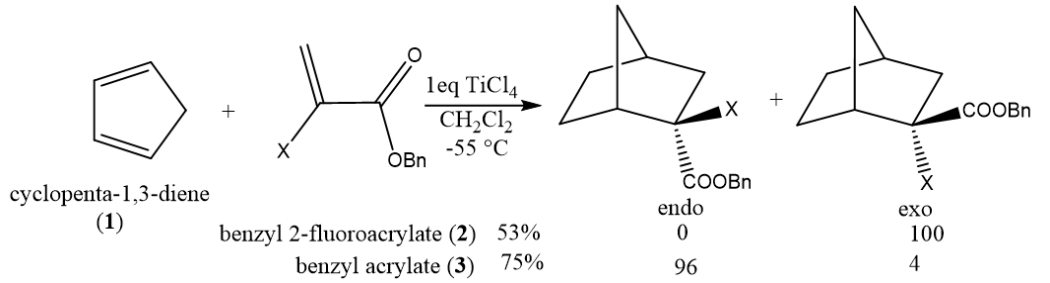

Scheme 3

Quantum methods are theoretical approaches based on the principles of quantum mechanics for understanding and predicting the behavior of molecular and atomic systems[13]. These methods are used to solve the fundamental equations that describe the behavior of subatomic particles, taking into account their quantum aspects, such as wave-particle duality and probability[14]. These methods are essential for understanding the electronic properties of molecules, chemical reactions, and for accurately predicting the behavior of complex quantum systems, which is crucial in many scientific fields. Specific methods, such as the Hartree-Fock method, Møller-Plesset (MP) perturbation theory and DFT, are widely used in quantum chemistry to study molecular structures, chemical reactions and the electronic properties of compounds[15-18]. Very recently, and within the framework of DFT, a theory has been proposed for chemical reactivity called MEDT[19].

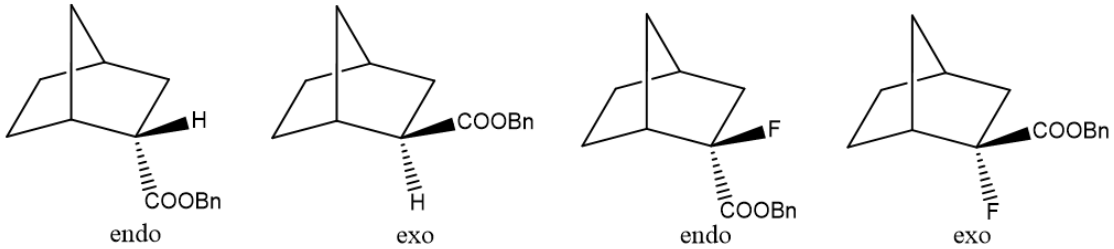

Fig. 1. The product undertaken carried out against corona and HIV viruses and compared to AZT and Vidresc

In this survey, Molecular Electron Density Theory (MEDT) was employed to investigate the stereoselectivity and elucidate the mechanism of the cycloaddition reaction, both catalyzed and non-catalyzed, between the compounds

cyclopenta-1,3-diene with benzyl acrylate and benzyl 2-fluoroacrylate[12]. Simultaneously, a docking analysis was undertaken carried out against corona and HIV viruses in order to predict the impact of stereochemistry and the influence of fluorine on the affinity and pharmacological properties of the products studied and compared to AZT and Nirmatrelvir.

2. Calculation method

The B3LYP/DFT method, applied with the SDD base[20], was used to perform calculations using Gaussian 09 software [21]. This approach was used to identify transition states (TS) by verifying the existence of a singular imaginary frequency. The use of IRC (Internal Reaction Coordinate) was also crucial in assessing the reaction trajectory, offering valuable insights into the progression from initial to final state[22]. In addition, the IRC facilitated understanding of the intermediate steps and activation barriers associated with each transition. In order to take into account, the impact of the solvent on the optimized structures, Tomas' PCM polarizable continuum model was integrated, enriching the accuracy of the calculations by considering the effects of the surrounding medium[23]. This rigorous methodological approach, combining DFT, IRC and the continuum model, offers an in-depth understanding of reaction mechanisms, with specific consideration of solvent influences on the transitional states and molecular structures involved in the reaction studied[24].

Understanding the electronic behavior of molecules is based on key concepts such as electronic chemical potential, chemical hardness, global electrophilicity index and nucleophilicity index[25]. Chemical electron potential is a measure of the energy required to add an electron to a system, providing information on the system's ability to accept electrons. Chemical hardness, on the other hand, is a measure of a system's resistance to changes in electron density, reflecting its stability. Global electrophilicity and nucleophilicity indices are crucial parameters in the prediction of chemical reactions. The overall electrophilicity index assesses a molecule's ability to act as an electron acceptor, while the nucleophilicity index measures a molecule's ability to act as an electron donor[25].

3. Result and discussion

3.1. Global indices

The global indices, namely chemical potential, chemical hardness, electrophilic indices, and nucleophilic indices catalyzed and not catalyzed of the cyclopent-3-diene reactants with benzyl acrylate and benzyl 2-fluoroacrylate, are compiled in Table 1.

Table 1. Chemical potential μ, chemical hardness η, electrophilic indices ω, and nucleophilic indices N, catalyzed and not catalyzed of the cyclopent-3-diene reactants with benzyl acrylate and benzyl 2-fluoroacrylate. (The values are given in eV)

System	μ	η	ω	N
1	-3.25	5.35	0.98	3.43
2	-4.59	4.36	2.42	2.58
2-Cat	-5.79	3.22	5.21	1.94
3	-4.32	4.59	2.03	2.73
3-Cat	-5.93	2.52	6.97	2.16

Table 1 presents various chemical descriptors for different systems involving cyclopent-3-diene reactants with benzyl acrylate and benzyl 2-fluoroacrylate. Let's analyze the data:

The chemical potential (μ) of -3.25 for System 1 is higher than that of the other systems, indicating that the electron transfer will occur from cyclopent-3-diene to the other reactants. The use of the catalyst reduces the hardness value of systems 2, 3-Cat, 3 and 3-Cat, making them highly reactive. The electrophilic power of cyclopent-3-diene is very small compared to other systems, and the use of the catalyst increases this power. The nucleophilic index of cyclopenta-3,1diene is very high compared to other reactants. In conclusion from this table, the cyclopent-3-diene reactant behaves as a nucleophile, while the other systems behave as electrophiles.

3.2. The Parr functions and ELF of the reactants

Parr functions are derived from density functional theory-based quantities such as electron density and its derivatives, as proposed in 2013 by Domingo[26]. They play a crucial role in studying local reactivity indices, providing information about the reactivity of specific regions within a molecule. The use of Parr functions in local reactivity refers to their application in understanding and analyzing the local reactivity of molecules. Figure 2 illustrates the Parr functions of benzyl acrylate and benzyl 2-fluoroacrylate under different conditions, both with and without a catalyzer (**2, 2-Cat, 3 and 3-Cat**). The Parr functions, derived from density functional theory, offer a detailed depiction of the electronic structure and reactivity of these compounds. The comparison between the two sets of data, with and without the catalyzer, provides insights into the impact of the catalyzer on the Parr functions and, consequently, on the electronic properties and reactivity of benzyl acrylate and benzyl 2-fluoroacrylate (**2, 2-Cat, 3 and 3-Cat**). This analysis aids in understanding the role of the catalyzer in influencing the electronic behavior of the compounds, offering valuable information for chemical and catalytic processes.

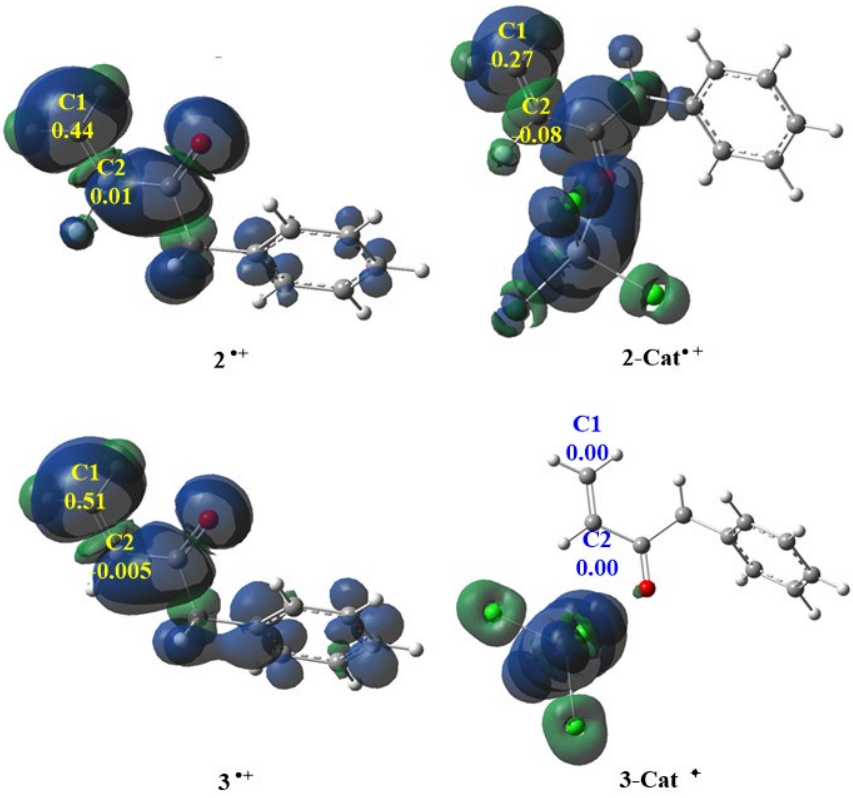

Fig. 2. Parr functions of benzyl acrylate and benzyl 2-fluoroacrylate with and without catalyzer (**2, 2-Cat, 3 and 3-Cat**)

The data from the Parr electrophilic functions for reactant 2 reveal that carbon C1 has a value of 0.44, while carbon C2 has a value of 0.04. When replacing the fluorine atom with a hydrogen atom, there is an increase in the Parr electrophilic value for the C1 center, reaching 0.51. The use of $TiCl_4$ as a catalyst in conjunction with reactant 2 leads to a decrease in the Parr electrophilic value for the C1 center, which reaches 0.27. However, the use of $TiCl_4$ with reactant 3 results in the cancellation of the Parr electrophiles. In summary, the analysis of Parr electrophilic functions suggests that the first bond will form on carbon C1, highlighting the significant influence of substitutions and catalysts on the electronic reactivity of the compound.

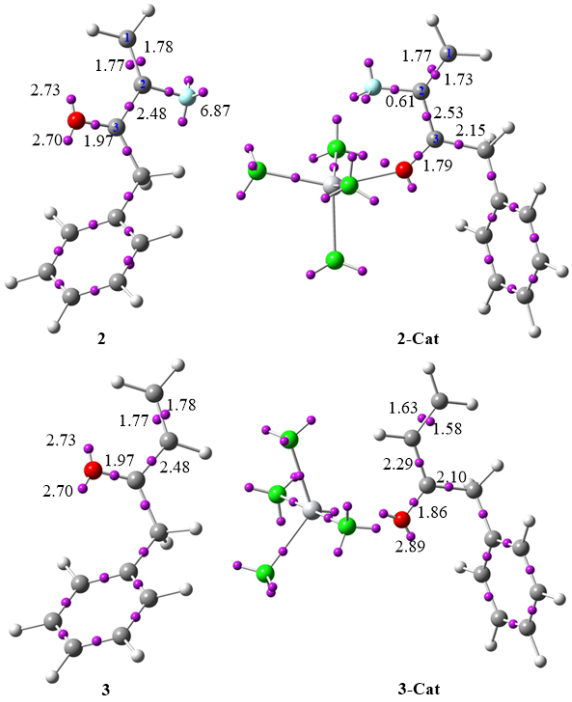

Fig. 3. The electron density basins and their values for benzyl acrylate and benzyl 2-fluoroacrylate with and without the catalyst (2, 2-Cat, 3, and 3-Cat)

To characterize the electronic distribution of the reactants, an in-depth ELF study was undertaken. **Fig. 3** consolidates the electronic basins of the alkenes, both in the presence and absence of a catalyst. This analysis allows for a detailed exploration of electron localization in these molecules, providing valuable insights into their electronic behavior, notably the influence of the catalyst and fluorine atom on the electronic distribution.

In the structure of reactant 2, careful observation reveals the presence of significant electron basins, including: V(C1,C2)=1.78e, V'(C1,C2)= 1.77e, V(C2,C3)= 2.48e, V(C3,O)= 2.73e, and two monosynaptic basins V(O)= 2.73e and V'(O)= 2.70e. The replacement of the fluorine atom with a hydrogen atom at position C2 does not cause any change in these same basins.

The introduction of $TiCl_4$ in conjunction with reactant 3 has a significant influence on the electron distribution. A decrease is observed in the values of bisynaptic basins: V(C1,C2)= 1.63e, V'(C1,C2)= 1.58e, V(C2,C3)= 2.29e, while the basin V(C3,O)= 2.73e increases and reaches 1.86e. The $TiCl_4$ catalyst does not induce major changes in the electron distribution of reactant 2; however, there is a slight modification in the values of bisynaptic basins V(C1,C2)and V'(C1,C2), totaling 3.50e. Therefore, the $TiCl_4$ catalyst attracts electrons from molecules 2 and 3, thereby imparting increased reactivity to these molecules. These results highlight the importance of catalyst choice in manipulating electron distribution and, by extension, in modulating molecular reactivity.

3.3. Energy Analysis of Cycloaddition Reaction Pathways of Cyclopenta-1,3-Diene with Benzyl-acrylate and Benzyl-2-Fluoroacrylate with and without catalyst

The reactants used in this study are non-symmetrical acrylates. Therefore, two pathways related to stereoselectivity (endo and exo) are conceivable. The different cycloaddition reaction pathways between cyclopenta-1,3-diene with benzyl acrylate and benzyl-2-fluoroacrylate, with or without a catalyst, are depicted in Scheme 4. The energy profiles are presented in **Fig. 4** and **Fig. 5**, while detailed calculations are listed in Tables S1, S2, S3, and S4.

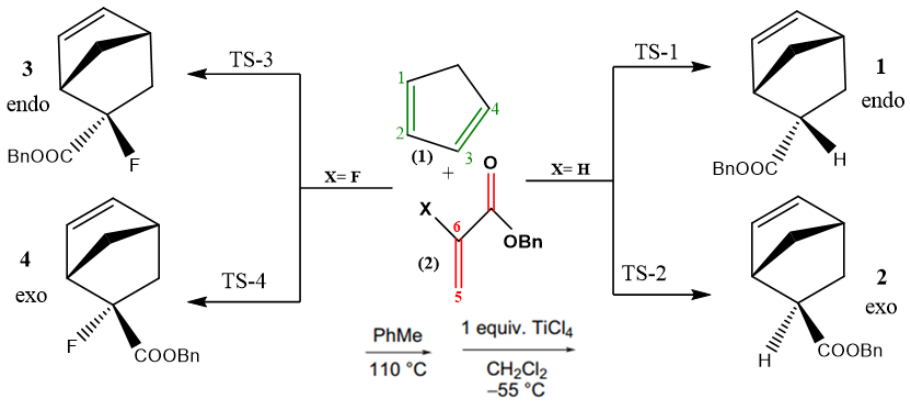

Scheme 4. Cycloaddition Reaction Pathways of Cyclopenta-1,3-Diene with Benzyl-acrylate and Benzyl-2-Fluoroacrylate with and without catalyst

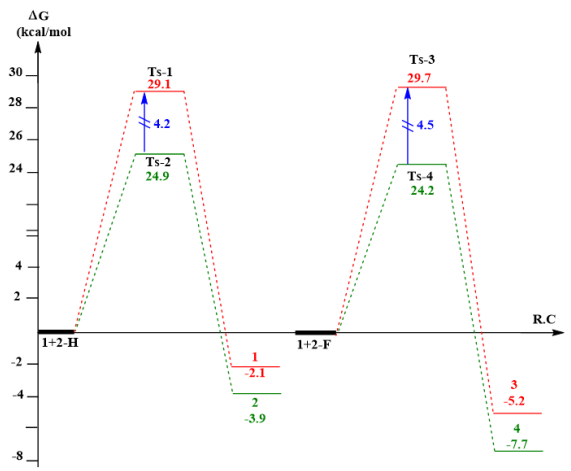

Fig. 4. Alternative chemical routes involving cyclopenta-1,3-diene with benzyl acrylate and benzyl-2-fluoro acrylate none catalysis

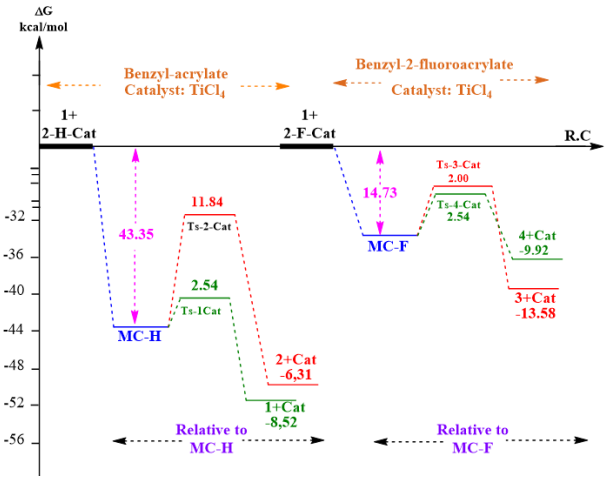

Fig. 5. Chemical reaction pathways between cyclopenta-1,3-diene with benzyl acrylate and benzyl-2-fluoro acrylate catalyzed by titanium tetrachloride

Fig. 4 provides insight into the energetics of the cycloaddition reactions involving cyclopenta-1,3-diene and benzyl acrylate. The negative values of Gibbs free energy (ΔG) signify the thermodynamic favorability of these reactions. Notably, the ΔG values for the formation of products 1 and 2 are -2.10 kcal/mol and -3.90 kcal/mol, respectively, indicating that product 2 is thermodynamically preferred. Furthermore, the transition states "Ts-1" and "Ts-2" exhibit high energy barriers, with ΔG values of 29.1 and 24.9, respectively. These barriers suggest significant activation energy requirements for the formation of these transition states. The relatively higher energy barrier associated with "Ts-1" indicates a more challenging transition state compared to "Ts-2". Consequently, the kinetic favorability of product 2, as indicated by the lower energy barrier, aligns with experimental observations. This analysis underscores the importance of considering both thermodynamic and kinetic factors in understanding product formation in cycloaddition reactions.

In **Fig. 4**, the values of Gibbs free energy (ΔG) for different cycloaddition reaction pathways between cyclopenta-1,3-diene and benzyl-2-fluoroacrylate are analyzed. The data reveal that the transition Ts-3 has a ΔG value of 29.7, suggesting a high energy barrier for this step. However, despite this energy barrier, product 3 exhibits a ΔG value of -5.2, indicating that its formation is thermodynamically favorable. Similarly, transition Ts-4 has a ΔG value of 24.2, also indicating an energy barrier for this step. Nevertheless, product 4 shows a ΔG value of -7.7, revealing formation that is both thermodynamically and kinetically favorable. These results confirm consistency with experimental observations and highlight the importance of both thermodynamic and kinetic aspects in understanding cycloaddition reactions.

The analysis of Gibbs free energy (ΔG) values in **Fig. 5** provides crucial insights into the reaction steps and catalytic products associated with the chemical process between cyclopenta-1,3-diene and benzyl acrylate catalyzed by titanium tetrachloride. In this context, the negative ΔG values observed for the "1-Cat" and "2-Cat" products indicate that the corresponding reactions are spontaneous, meaning they are thermodynamically favorable. Additionally, 1-Cat exhibits higher free reaction energy than 2-Cat, indicating that the 1-Cat products is thermodynamically very favorable. This suggests that these reactions can occur efficiently with a release of energy. Conversely, the activation energies for "Ts-1-Cat" and "Ts-2-Cat," at 2.54 kcal/mol and 11.84 kcal/mol, respectively, indicate that the 1-Cat product (**endo product**) is thermodynamically and kinetically very favorable, and the gap between the two transition states becomes larger than in the un-catalyzed reaction, indicating an increase in selectivity. This analysis of ΔG values also allows for the evaluation of the stability and viability of different transition states and catalytic products associated with the reaction. In conclusion of this analysis, reaction pathway 1 predominates, which aligns well with experimental results.

Fig. 5 depicts also the data on changes in free energy (ΔG) for the chemical reaction pathways between cyclopenta-1,3-diene and benzyl-2-fluoro acrylate catalyzed by titanium tetrachloride. The formation reaction of the product 3-Cat is highly exothermic, with a ΔG value of -13.58 kcal/mol, indicating a significant release of energy during its formation, similarly, the formation reaction of the product 4-Cat is exothermic, although to a lesser extent than the preceding reaction, with a ΔG value of -9.92 kcal/mol. The negative ΔG values for the catalyzed products ("3-Cat" and "4-Cat") indicate that these reactions are spontaneous and that the 3-Cat product is thermodynamically favorable. Conversely, the activation energies "Ts-3-Cat" and "Ts-4-Cat" are 2.00 kcal/mol and 1.90 kcal/mol, respectively, indicating that the Ts-4-Cat product is kinetically favored. However, these activation energies remain relatively low, suggesting that the presence of the catalyst facilitates these transitions. In conclusion, catalysis appears to play a crucial role in determining reaction pathways, by reducing the energy barriers to reach the 4-Cat product (exo product). This result is in good agreement with experimental findings. Therefore, it can be concluded that the exo product (4-Cat) is obtained under kinetic control.

3.4. ELF analysis of the cycloaddition reactions between cyclopenta-1,3-diene and benzyl acrylate as well as benzyl-2-fluoro acrylate

The Electron Localization Function (ELF) Analysis is a powerful method used in theoretical chemistry to understand complex reaction mechanisms. This approach allows visualization of electron localization within a molecule, which is essential for understanding chemical interactions and electron rearrangements occurring during a reaction. ELF analyses can identify sites where electrons are localized during the formation and breaking of chemical bonds, as well as regions of increased electron density. This provides valuable insights into key steps of the reaction mechanism, such as the formation of reaction intermediates, transition states, and final products. In this section, an ELF study was conducted to understand the mechanism of each reaction. **Table S5** and **Table S6** seem to represent the values of basins between atoms involved in the formation of new bonds during the cycloaddition reaction without catalysts, while the relevant structures are shown in **Fig. 6** and **Fig. 7**. On the other hand, **Table S7** and **Table S8** appear to present the values of basins between atoms during the same reaction but with the addition of a catalyst, and the important structures are illustrated in **Fig. 8** and **Fig. 9**. From **Table S5** it can see that the values of V(C1, C2), V(C3, C4), and V(C1, C4) represent the basins between different carbon atoms. These values generally decrease when going from the 1-H structure to the 4-H structure, indicating a change in the nature of the carbon-carbon bonds in the molecule. Similarly, the value of V(C10, C11) follows a similar trend, with smaller basins observed in the 4-H base compared to the 1-H base. In the 3-H structure, the appearance of monosynaptic basins V(C3) and V(C11) results in a significant increase in their values from the 3-H structure to the 4-H structure, respectively reaching 0.49e and 0.42e. These two monosynaptic basins merge to form the first bond C3,C11 with a value of V(C3,C11)=1.20e. In the 6-H structure, two monosynaptic basins appear, carried by the carbon atoms C2 and C10, with

values of V(C2) equal to 0.20e and V(C10) equal to 0.47e. The V(C2) and V(C10) basins combine to form the second bond, with an electronic density of V(C2,C10) equal to 1.10e. According to this analysis, it can be concluded that the mechanism followed by the cycloaddition reaction between cyclopenta-1,3-diene and benzyl is asynchronous.

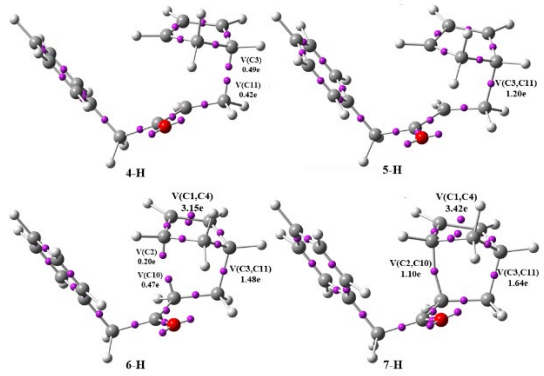

Fig. 6. The relevant structure

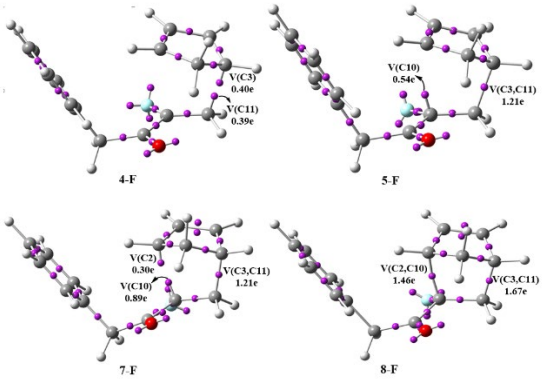

Fig. 7. The relevant structure

From **Table S6**, it is evident that the same remarks made in the previous reaction show that the values of V(C1, C2), V(C3, C4), and V(C1, C4) decrease globally as we move from structure 1-F to structure 4-F, indicating a change in the type of carbon-carbon bonds within the molecule. Similarly, the value of V(C10, C11) also follows a similar trend, with smaller basins observed in base 4-F compared to base 1-F. In structure 3-F, the appearance of monosynaptic basins V(C3) and V(C11) results in a significant increase in their values in the 4-F configuration, reaching 0.40e and 0.39e respectively. The fusion of these two monosynaptic basins leads to the formation of the first bond in structure 5-F, with a value of 1.21e for the bassin V(C3, C11). In this same structure, a new monosynaptic basin, V(C10), appears with a value of 0.54e. In structure 7-F, the value of this basin increases to 0.89e, and another monosynaptic basin, V(C2), appears with a value of 0.30e. In structure 8-F, the monosynaptic basins V(C10) and V(C2) are merged to form the second bond with a value of 1.46e. This shows that the mechanism followed by the cycloaddition reaction between cyclopenta-1,3-diene with benzyl-2-fluoro acrylate is asynchronous.

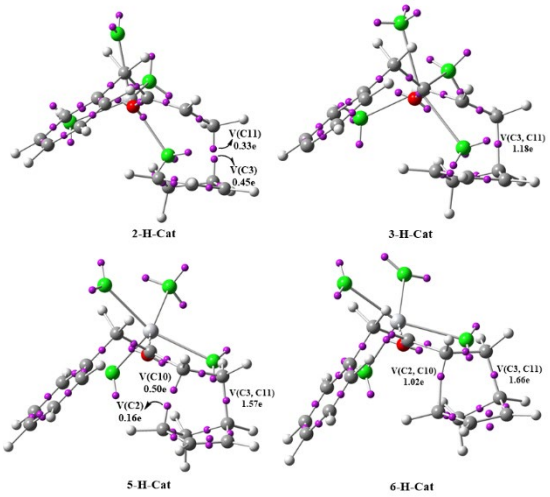

Fig. 8. The relevant structure

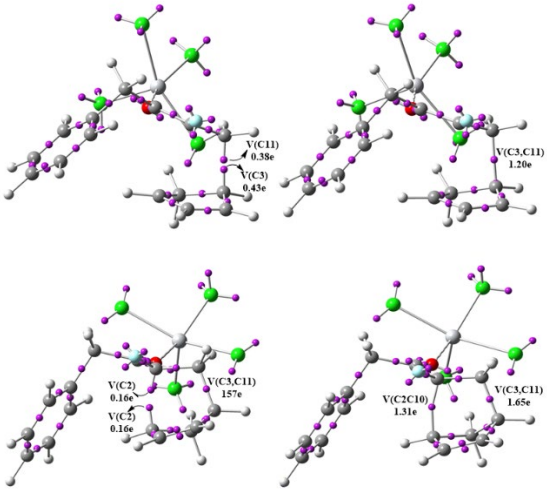

Fig. 9. The relevant structure

Table S7 appears to represent the values of electron basins within these fragments. It is notable that the values of the V(C1,C2) basins, which connect carbons C1 and C2, decrease progressively from 3.21e to 2.18e, suggesting a reduction in electron density between these carbons. Similarly, the values of the V(C3,C4) basins also decrease from 3.19e to 2.05e, indicating a similar reduction in electron density between these carbons. However, the values of the V(C1,C4) basins increase from 2.25e to 3.25e. Additionally, the values of the V(C10,C11) basins decrease from 3.10e to 1.97e, demonstrating a significant decrease in electron density between these carbons. These observations suggest that double bonds are becoming single bonds while single bonds are becoming double bonds, consequently leading to changes in carbon-carbon bonds within the molecule. In structure 2-H-Cat, there is an emergence of two monosynaptic basins carried by C3 and C11, with values of 0.45e and 0.33e respectively. These two basins merge to form the first bond with a value of 1.18e. Additionally, in structure 2-H-Cat, there is an emergence of two monosynaptic basins located on C2 and C10, with respective values of 0.16e and 0.50e. These two basins combine to form the second bond, which has a value of 1.02e. Consequently, the mechanism of the cycloaddition reaction between cyclopenta-1,3-diene with benzyl acrylate catalyzed by $TiCl_4$ follows an asynchronous mechanism.

According to **Table S8**, we notice that the values of the V(C1,C2) basins, which connect carbons C1 and C2, gradually decrease from 3.18e to 2.19e. Similarly, the values of the V(C3,C4) basins also decrease from 3.17e to 2.05e, indicating a similar decrease in electron density between these carbons. However, the values of the V(C1,C4) basins increase from 2.26e to 3.21e. Additionally, the values of the V(C10,C11) basins decrease from 3.10e to 2.09e. These observations thus lead to changes in the carbon-carbon bonds within the molecule, suggesting that double bonds are converting into single bonds while single bonds are becoming double bonds. In structure 2-F-Cat, the emergence of two monosynaptic basins carried by C3 and C11 is observed, with respective values of 0.43e and 0.38e. These two basins combine to form the first bond with a value of 1.20e. In structure 3-F-Cat, the emergence of two monosynaptic basins on C2 and C10 is noted, with respective values of 0.16e and 0.82e. These two basins unite to form the second bond, which displays a value of 1.31e. Consequently, the mechanism of the cycloaddition reaction between cyclopenta-1,3-diene with benzyl-2-fluoro acrylate catalyzed by TiCl4 follows an asynchronous mode.

3.4. Exploring the Binding Affinity of a Product under Study towards COVID-19 and HIV-1 Proteins

Molecular docking is a crucial step in modern pharmaceutical research focused on identifying new candidate molecules for therapeutic purposes. This approach involves predicting and analyzing how a specific molecule spatially interacts with a given biological target, typically a protein. By using advanced computational techniques such as molecular modeling and molecular dynamics simulation, molecular docking enables visualization of potential binding sites, the forces involved, and the characteristics of molecular interaction. This method is essential for the systematic design of drugs, facilitating the exploration of promising chemical compounds by precisely targeting the active sites of proteins involved in various pathologies. Thus, molecular docking represents a powerful approach for the design and improvement of drugs, leading to significant advancements in the development of more precise and effective therapies. In this innovative study, we examine the interaction between a specific derivative of benzyl-2-fluorobicyclo[2.2.1]heptane-2-carboxylate (Figure 2) and proteins associated with the Covid-19 virus and HIV. Our approach aims to elucidate the underlying molecular mechanisms of the binding between these compounds and these viral proteins. This study promises to provide significant insights into the understanding of molecular interactions between the studied derivatives of heptane-2-carboxylate and the key proteins of the Covid-19 and HIV viruses, thereby opening new perspectives in the development of potential therapies.

The data presented in **Table 2** provide an overview of the energy affinities (expressed in kcal/mol) between different ligands, including 1, 2, 3, 4, Nirmatrelvir, and L'AZT, towards proteins associated with Covid-19 and HIV. These affinity values are crucial for assessing the potential binding strength between each ligand and the target proteins. Additionally, **Fig. 10** complements this analysis by providing a visual representation of molecular interactions in two and three dimensions for specific ligands, 1, 4, Nirmatrelvir, and L'AZT. This visualization allows for a better understanding of the spatial interaction patterns between these compounds and the studied proteins, thus paving the way for significant insights in the context of drug design and therapeutic research.

Table 2. The energy binding affinities (in kcal/mol) of different ligands, specifically 01, 2, 3, 4, Nirmatrelvir, and L'AZT

Molecule	HIV affinity (kcal/mol)	Covid-19 affinity (kcal/mol)
1	-4.9	-6.4
2	-4.5	-5.2
3	-4.8	-5.9
4	-5.2	-6.1
AZT	-4.9	------
Nirmatrelvir	------	-6.2

Table 2 presents a detailed analysis of the energetic affinities between different ligands and the Covid-19 protein. Each ligand, including 1, 2, 3, 4, and Nirmatrelvir, is associated with a specific energy affinity value. Negative values indicate favorable affinity, where lower values suggest potentially stronger binding between the ligand and the protein. This data analysis allows for comparing each ligand's ability to bind to the Covid-19 protein, providing crucial insights for evaluating their potential as inhibitors or therapeutic compounds. For example, ligand 1 exhibits the lowest affinity, indicating potentially stronger binding with the Covid-19 protein compared to other ligands. This in-depth analysis assists in guiding the selection of promising ligands for further studies as potential therapeutic agents. From this analysis, it can be inferred that the inclusion of the fluorine atom does not improve the affinity of the studied fluorinated products; Ligand 1 has shown promising affinity with the Covid-19 protein in this study. This observation underscores its potential as a candidate for the development of a drug against Covid-19. Further research on ligand 1 could consolidate this preliminary finding by assessing its ability to specifically inhibit the functions or propagation of the SARS-CoV-2 virus. These studies could also explore the molecular signaling pathways involved in the interaction between ligand 1 and the viral protein, thus paving the way for innovative therapeutic approaches to combat Covid-19.

Table 2 also offers a thorough examination of the energetic affinities exhibited by various ligands towards the human immunodeficiency virus (HIV). The ligands under investigation encompass 1, 2, 3, 4, and Zidovudine. All recorded energy affinity values were negative, indicating a favorable interaction between the ligands and HIV. Lower values imply a more robust binding between the ligand and HIV. By scrutinizing these data, we can assess the binding capability of each ligand

to HIV, thus providing crucial insights into their potential as inhibitors or therapeutic agents. For instance, ligand 4 demonstrates the highest affinity, suggesting a particularly potent interaction with HIV compared to the other ligands listed. This comprehensive analysis aids in selecting promising ligands for further exploration as potential therapeutic candidates. Specifically, ligand 4 exhibits significantly high affinity for human immunodeficiency virus (HIV), making it a major subject of interest for further research. Its strong affinity suggests a robust ability to bind to HIV viral proteins, which could potentially lead to the development of new, more effective anti-retroviral drugs. Additional studies on ligand 4 could provide detailed insight into its binding mechanisms with HIV, as well as exploring its therapeutic implications and potential for developing improved treatments against HIV.

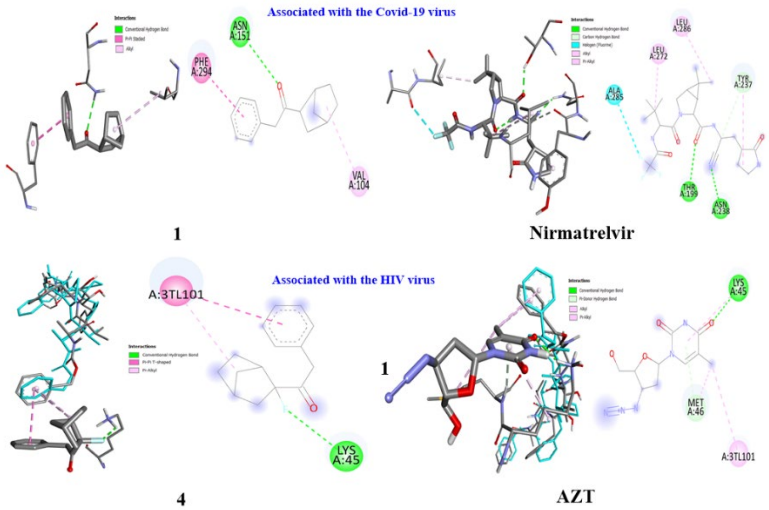

Fig. 10. A graphical depiction of molecular interactions in both two and three dimensions involving compounds 1, 4, AZT, and nirmatrelvir

4. Conclusion

The investigation delved into the cycloaddition reactions involving cyclopenta-1,3-diene and benzyl acrylate, as well as benzyl 2-fluoroacrylate, both with and without the catalyst (TiCl4). This exploration employed the Molecular Electron Density Theory (MEDT) at the DFT/B3LYP/SDD calculation level. This methodology allowed for a comprehensive analysis of the energy profiles linked to these reactions, thereby providing valuable insights into their mechanisms and stereochemical selectivity. The findings gleaned from the energy profiles suggest that these reactions exhibit stereoselectivity, showing a preference for the formation of specific stereoisomers over others. Furthermore, the inclusion of $TiCl_4$ as a catalyst appears to enhance the selectivity of these reactions, in line with experimental observations. Additionally, a docking analysis was conducted to forecast how stereochemistry and the presence of specific atoms, such as fluorine, might impact their binding affinity to viral proteins associated with SARS-Covid-19 and HIV, in addition Ligand 4's high affinity for HIV makes it a prime candidate for further research, potentially leading to improved antiretroviral medications, while ligand 1's promising affinity with the Covid-19 protein underscores its potential as a candidate for Covid-19 drug development. Additional investigations into ligand 1 could bolster its candidacy by exploring its ability to inhibit SARS-CoV-2 and understanding its molecular interactions, offering avenues for innovative therapeutic strategies against Covid-19.

References

1. Lenci E., Menchi G., Saldívar-Gonzalez F. I., Medina-Franco J. L., and Trabocchi A. (**2019**) Bicyclic acetals: biological relevance, scaffold analysis, and applications in diversity-oriented synthesis. *Org. Biomol. Chem., 17*, 1037-1052. https://doi.org/10.1039/C8OB02808G
2. Phang Y., Wang X., Lu Y., Fu W., Zheng C., Xu H. (**2020**) Bicyclic polyprenylated acylphloroglucinols and their derivatives: structural modification, structure-activity relationship, biological activity and mechanism of action. *Eur. J. Med. Chem., 205*, 112646. https://doi.org/10.1016/j.ejmech.2020.112646
3. Wang H., Willershäuser M., Karlas A., Gorpas D., Reber J., Ntziachristos V., Maurer S., Fromme T., Li Y., Klingenspor M. (**2019**) A dual Ucp1 reporter mouse model for imaging and quantitation of brown and brite fat recruitment. *Mol. Metab., 20*, 14-27. https://doi.org/10.1016/j.molmet.2018.11.009
4. Kumar S., Sharma S., Chattopadhyay S. K. (**2013**) The potential health benefit of polyisoprenylated benzophenones from Garcinia and related genera: Ethnobotanical and therapeutic importance. *Fitoterapia, 89*, 86-125. https://doi.org/10.1016/j.fitote.2013.05.010

5. Hall D. G., Rybak T., Verdelet T. (**2016**) Multicomponent Hetero-[4 + 2] Cycloaddition/Allylboration Reaction: From Natural Product Synthesis to Drug Discovery. *Acc. Chem. Res., 49* (11), 2489-2500. https://doi.org/10.1021/acs.accounts.6b00403
6. Ouled Abdelhak A., Barhoumi A., Zeroual A. (**2023**) A mechanism study and an investigation of the reason for the stereoselectivity in the [4+2] cycloaddition reaction between cyclopentadiene and gem-substituted ethylene electrophiles. *Scientiae Radices*, 2(3), 217-228. https://doi.org/10.58332/scirad2023v2i3a01
7. Mei H., Han J., Fustero S., Medio-Simon M., Sedgwick D. M., Santi C., Ruzziconi R., Soloshonok V. A. (**2019**) Fluorine-Containing Drugs Approved by the FDA in 2018. *Chem. Eur. J., 25*, 11797. https://doi.org/10.1002/chem.201901840
8. Wen L., Li B., Zou Z., Zhou N., Sun C., Feng P., Li H. (**2024**) Direct electrochemical difluorination and azo-fluorination of gem-difluorostyrenes. *Org. Chem. Front., 11* (1), 142-148. https://doi.org/10.1039/D3QO00599B
9. Henary E., Casa S., Dost T. L., Sloop J. C., Henary M. (**2024**) The Role of Small Molecules Containing Fluorine Atoms in Medicine and Imaging Applications. *Pharmaceuticals, 17* (3), 281. https://doi.org/10.3390/ph17030281
10. Wang L., Zhu X., Wang B., Wang Y., Wang M., Yang S., Su C., Chang J., Zhu B. (**2024**) Design, Synthesis, and Activity Evaluation of Fluorine-Containing Scopolamine Analogues as Potential Antidepressants. *J. Med. Chem.*, 10.1021/acs.jmedchem.3c01970
11. Shabir G., Saeed A., Zahid W., Naseer F., Riaz Z., Khalil N., Muneeba, Albericio F. (**2023**) Chemistry and Pharmacology of Fluorinated Drugs Approved by the FDA (2016–2022). *Pharmaceuticals, 16*(8), 1162. https://doi.org/10.3390/ph16081162
12. D., Hellel, F., Chafaa, A. K. Nacereddine (**2023**) Synthesis of tetrahydroquinolines and quinoline derivatives through the Lewis acid catalysed Povarov reaction: A comparative study between multi step and multi-component methods. *Scientiae Radices, 2*(3), 295-308. https://doi.org/10.58332/scirad2023v2i3a05
13. Dresler E., Wróblewska A., Jasiński R. (**2023**) Understanding the Molecular Mechanism of Thermal and LA-Catalysed Diels–Alder Reactions between Cyclopentadiene and Isopropyl 3-Nitroprop-2-Enate. *Molecules, 28*, 5289. https://doi.org/10.3390/molecules28145289
14. Jasiński R. (**2021**) On the Question of Stepwise [4+2] Cycloaddition Reactions and Their Stereochemical Aspects. *Symmetry, 13*, 1911. https://doi.org/10.3390/sym13101911
15. Ameur S., Barhoumi A., Ríos-Gutiérrez M., Ouled Aitouna A., El Alaoui El Abdallaoui H., Mazoir N., Elalaoui Belghiti M., Syed A., Zeroual A., Domingo L. R. (**2023**) A MEDT study of the mechanism and selectivity of the hetero-Diels–Alder reaction between 3-benzoylpyrrolo[1,2-c][1,4]-benzoxazine-1,2,4-trione and vinyl acetate. *Chem. Heterocycl. Compd., 59*(3), 165-170.
16. Barhoumi A., Ourhriss N., Elalaoui Belghiti M., Chafi M., Syed A., Eswaramoorthy R., Verma M., Zeroual A., Zawadzińsk K., Jasiński R. (**2023**) 3-Difluormethyl-5-carbomethoxy-2,4-pyrazole: Molecular mechanism of the formation and molecular docking study. *Curr. Chem. Lett., 12*, 477-488. https://doi.org/10.5267/j.ccl.2023.3.008
17. Raji H., Ouled Aitouna A., Barhoumi A., Chekroun A., Zeroual A., Syed A., Elgorban A. M., Verma M., Benharref A., Varma R. S. (**2023**) Antiviral docking analysis, semisynthesis and mechanistic studies on the origin of stereo- and chemoselectivity in epoxidation reaction of α′-trans-Himachalene. *J. Mol. Liq.*, 385, 122204. https://doi.org/10.1016/j.molliq.2023.122204
18. Barhoumi A., Ryachi K., Elalaoui Belghiti M., Chafi M., Tounsi A., Syed A., El Idrissi M., Wong L. S., Zeroual A. (**2023**) Chromatography Scrutiny, Molecular Docking, Clarifying the Selectivities and the Mechanism of [3+2] Cycloaddition Reaction between Linallol and Chlorobenzene-Nitrile-oxide. *J. Fluoresc.*, https://doi.org/10.1007/s10895-023-03411-z
19. Domingo L. R., Ríos-Gutiérrez M., Pérez P. (**2016**) Applications of the Conceptual Density Functional Theory Indices to Organic Chemistry Reactivity. *Molecules, 21*, 748. https://doi.org/10.3390/molecules21060748
20. Jasiński R. (**2016**) First example of stepwise, zwitterionic mechanism for bicyclo[2.2.1]hept-5-ene (norbornene) formation process catalyzed by the 1-butyl-3-methylimidazolium cations. *Monatsh Chem., 147*, 1207-1213. https://doi.org/10.1007/s00706-016-1735-5
21. Frisch M. J., Trucks G. W., Schlegel H. B., Scuseria G. E., Robb M. A., Cheeseman J. R., Scalmani G., Barone V., Mennucci B., Petersson G. A., Nakatsuji H., Caricato M., Li X., Hratchian H. P., Izmaylov A. F., Bloino J., Zheng G., Sonnenberg J. L., Hada M., Ehara M., Toyota K., Fukuda R., Hasegawa J., Ishida M., Nakajima T., Honda Y., Kitao O., Nakai H., Vreven T., Montgomery J. A. Jr., Peralta J. E., Ogliaro F., Bearpark M., Heyd J. J., Brothers E., Kudin K. N., Staroverov V. N., Kobayashi R., Normand J., Raghavachari K., Rendell A., Burant J. C., Iyengar S. S., Tomasi J., Cossi M., Rega N., Millam J. M., Klene M., Knox J. E., Cross J. B., Bakken V., Adamo C., Jaramillo J., Gomperts R., Stratmann R. E., Yazyev O., Austin A. J., Cammi R., Pomelli C., Ochterski J. W., Martin R. L., Morokuma K., Zakrzewski V. G., Voth G. A., Salvador P., Dannenberg J. J., Dapprich S., Daniels A. D., Farkas O., Foresman J. B., Ortiz J. V., Cioslowski J., Fox D. J. (**2009**) Gaussian 09, Revision A.02, Gaussian, Inc., Wallingford CT.
22. Deng L., Ziegler T. (**1994**) The determination of intrinsic reaction coordinates by density functional theory. *Int. J. Quantum Chem., 52*, 731-765. https://doi.org/10.1002/qua.560520406
23. Tomasi J., Cammi R., Mennucci B. (**1999**) Medium effects on the properties of chemical systems: An overview of recent formulations in the polarizable continuum model (PCM). *Int. J. Quantum Chem., 75*, 783-803. https://doi.org/10.1002/(SICI)1097-461X(1999)75:4/5<783::AID-QUA44>3.0.CO;2-G

24. Vogiatzis K. D., Polynski M. V., Kirkland J. K., Townsend J., Hashemi A., Liu C., Pidko E. A. (**2019**) Computational Approach to Molecular Catalysis by 3d Transition Metals: Challenges and Opportunities. *Chem. Rev., 119* (4), 2453-2523. https://doi.org/10.1021/acs.chemrev.8b00361
25. Ríos-Gutiérrez M., Saz Sousa A., Domingo L. R. (**2023**) Electrophilicity and nucleophilicity scales at different DFT computational levels. *J. Phys. Org. Chem., 36*(7), e4503. https://doi.org/10.1002/poc.4503
26. Domingo L. R., Pérez P., Sáez J. A. (**2013**) Understanding the local reactivity in polar organic reactions through electrophilic and nucleophilic Parr functions. *RSC Adv., 3*, 1486-1494. https://doi.org/10.1039/C2RA22886F